Sequential Salinomycin Treatment Results in Resistance Formation through Clonal Selection of Epithelial-Like Tumor Cells[1,2]

Florian Kopp*, Adam Hermawan*,
Prajakta Shirish Oak*, Vijay Kumar Ulaganathan[†],
Annika Herrmann*, Nefertiti Elnikhely[‡],
Chitra Thakur[†], Zhiguang Xiao[§], Pjotr Knyazev[§],
Beyhan Ataseven[¶], Rajkumar Savai[‡],
Ernst Wagner* and Andreas Roidl*

*Pharmaceutical Biotechnology, Department of Pharmacy, Ludwig-Maximilians-Universität München, Munich, Germany; [†]Department of Molecular Biology, "Cancer Metastasis Group", Max-Planck Institute of Biochemistry, Martinsried, Germany; [‡]Molecular Mechanisms in Lung Cancer, Max Planck Institute for Heart and Lung Research, Bad Nauheim, Germany; [§]Department of Molecular Biology, Max Planck Institute of Biochemistry, Martinsried, Germany; [¶]Department of Gynecology and Obstetrics, Rotkreuzklinikum Munich, Germany

Abstract

Acquiring therapy resistance is one of the major obstacles in the treatment of patients with cancer. The discovery of the cancer stem cell (CSC)–specific drug salinomycin raised hope for improved treatment options by targeting therapy-refractory CSCs and mesenchymal cancer cells. However, the occurrence of an acquired salinomycin resistance in tumor cells remains elusive. To study the formation of salinomycin resistance, mesenchymal breast cancer cells were sequentially treated with salinomycin in an *in vitro* cell culture assay, and the resulting differences in gene expression and salinomycin susceptibility were analyzed. We demonstrated that long-term salinomycin treatment of mesenchymal cancer cells resulted in salinomycin-resistant cells with elevated levels of epithelial markers, such as E-cadherin and miR-200c, a decreased migratory capability, and a higher susceptibility to the classic chemotherapeutic drug doxorubicin. The formation of salinomycin resistance through the acquisition of epithelial traits was further validated by inducing mesenchymal-epithelial transition through an overexpression of miR-200c. The transition from a mesenchymal to a more epithelial-like phenotype of salinomycin-treated tumor cells was moreover confirmed *in vivo*, using syngeneic and, for the first time, transgenic mouse tumor models. These results suggest that the acquisition of salinomycin resistance through the clonal selection of epithelial-like cancer cells could become exploited for improved cancer therapies by antagonizing the tumor-progressive effects of epithelial-mesenchymal transition.

Translational Oncology (2014) 7, 702–711

Introduction

The acquisition of chemoresistance represents one of the major obstacles in cancer treatment. Albeit early detection methods improved and novel treatment options emerged, resistance formation to chemotherapeutics remains an enormous challenge for cancer therapy. In breast cancer, 30% of all patients with breast cancer suffer a relapse associated with metastasis and chemoresistance. The response rates for classic chemotherapy including anthracyclines and taxanes drop to only 20% to 30% on disease progression, even though the response rates for first-line chemotherapy are up to 70%. Several resistance mechanisms, such as the up-regulation of ATP binding cassette transporters and the overexpression and constitutive activity of growth factor receptors or certain other proteins and enzymes like β-tubulin III and thioredoxin [1–4], have been identified over the last years. In addition, recent findings on intratumoral heterogeneity [5–7] suggest that clonal evolution and plasticity are important drivers of the long-term resistance formation to chemotherapy. With regard to this, cancer stem cells (CSCs) became important targets of therapeutic approaches as they give rise to resistant subpopulations and thus are assumed to be one of the major causes of relapse and therapy resistance. Gupta et al. have found salinomycin to be a selective inhibitor of CSC, being 100-fold more effective than paclitaxel, a commonly used chemotherapeutic breast cancer drug [8]. Subsequent studies in a variety of different cancer types including breast, blood, lung, pancreas, and colon have revealed diverse mechanisms of salinomycin action against CSC resulting in apoptosis and cell death [9–12]. Interestingly, in several recent studies, salinomycin has been reported to induce apoptosis in cisplatin-resistant cancer cells [13–15], to overcome ATP binding cassette transporter–mediated drug resistance in leukemia cells [16], and to sensitize cancer cells to different chemotherapeutic drugs [17,18], hence circumventing the resistance to classic chemotherapy. Therefore, treatment with salinomycin in addition to classic cancer therapy could greatly improve the prognosis of patients with cancer. Several case studies applying salinomycin in a clinical setting revealed beneficial effects in patients with exhausted therapy options [9]. Because of these promising results, it is of great interest to investigate resistance formation to salinomycin treatment as the occurrence and the potential underlying mechanisms of an acquired salinomycin resistance in cancer cells remain elusive.

In this study, we sought to investigate the resistance formation to long-term sequential salinomycin treatment in an *in vitro* cell culture assay. We found that repeated salinomycin treatment resulted in a clonal selection of cells displaying more epithelial traits and increased resistance to salinomycin. Of note, in syngeneic and transgenic mouse tumor models, we also observed the selection of epithelial-like cell clones.

Materials and Methods

Reagents

These primary antibodies against the following proteins were used: actin (I-19) (SC-1616; Santa Cruz Biotechnology, Dallas, Texas) for Western blot (WB); vimentin (D21H3) XP (#5741; Cell Signaling Technology, Boston, Massachusetts) for WB and *in vivo* immunohistochemistry (IHC)/immunofluorescence (IF); E-cadherin (24E10) (#3195; Cell Signaling Technology) for WB and *in vivo* IHC/IF; E-cadherin (DECMA-1) (ab11512; Abcam, Cambridge, UK) for *in vitro* IF; vimentin (V9) (SC-6260, Santa Cruz Biotechnology) for *in vitro* IF. Salinomycin (S6201) was obtained from Sigma-Aldrich, Munich, Germany.

Cell Culture

The breast (BT-474, MCF-7, MDA-MB-231, MDA-MB-436, and 4T1) and lung (NCI-H1299 and Lewis lung carcinoma) cancer cell lines were cultivated according to the supplier's instructions (ATCC).

Transfections

For miR-200c overexpression experiments, cells were transfected with either Pre-miR miRNA Precursor of hsa-miR-200c (pre-miR-200c; Ambion) or Pre-miR miRNA Negative Control (control; Ambion) using Lipofectamine 2000 (Invitrogen, Darmstadt, Germany) according to the manufacturer's protocol.

Quantitative Reverse Transcription–Polymerase Chain Reaction

Total RNA was isolated with the miRCURY RNA Isolation Kit (Exiqon, Vedbaek, Denmark) according to the manufacturer's instructions. miRNA or mRNA was reversely transcribed and subjected to quantitative reverse transcription–polymerase chain reaction (RT-PCR) as described previously [19]. All experiments were done in triplicate, and the following primers and hydrolysis probes (Roche, Penzberg, Germany) were used: E-cadherin (hsa), UPL Probe #35, left primer: CCCGGGA-CAACGTTTATTAC, right primer: GCTGGCTCAAGT-CAAAGTCC; vimentin (hsa): UPL Probe #56, left primer: GTTTCCCCTAAACCGCTAGG, right primer: AGCGAGAGTGG-CAGAGGA; zeb2 (hsa): UPL Probe #68, left primer: AAGCCAGGGA-CAGATCAGC, right primer: CCACACTCTGTGCATTTGAACT; Glycerinaldehyd-3-phosphat-Dehydrogenase (GAPDH) (hsa), UPL Probe #60, left primer: AGCCACATCGCTCAGACAC, right primer: GCCCAATACGACCAAATCC; E-cadherin (mmu): UPL Probe #18, left primer: ATCCTCGCCCTGCTGATT, right primer: ACCACCGTTCTCCTCCGTA; vimentin (mmu): UPL Probe #79, left primer: TGCGCCAGCAGTATGAAA, right primer: GCCTCAGAGAGGTCAGCAAA; zeb2 (mmu): UPL Probe #42, left primer: CCAGAGGAAACAAGGATTTCAG, right primer: AGGCCTGACATGTAGTCTTGTG; GAPDH (mmu): Universal ProbeLibrary Mouse GAPD Gene Assay (Roche); miR-200c stem loop primer (hsa and mmu): GTTGGCTCTGGTGC-AGGGTCCGAGGTATTCGCACCAGAGCCAACTCCATC; miR-200c forward primer: GCGTAATACTGCCGGGTAAT; universal reverse primer: GTGCAGGGTCCGAGGT.

Cell Lysis and Immunoblot Analysis

WB experiments were performed as described previously [19] using the respective antibodies from the Reagents section.

Cell Viability Assay

For cytotoxicity experiments, cells were seeded on 96-well plates at a density of 5000 cells per well. After 24 hours, cells were incubated with the respective drugs for 72 hours unless otherwise indicated. Subsequently, the CellTiter-Glo (Promega, Mannheim, Germany) assay was performed according to the manufacturer's protocol. Cell viability was normalized to the respective mock-treated control cells and presented as percent of control. Half maximal inhibitory concentration (IC_{50}) values for salinomycin were obtained from several different drug concentrations using GraphPad Prism software for analysis. All experiments were done in triplicate.

Long-Term In Vitro Salinomycin Treatment

MDA-MB-436 cells received a long-term pulsed salinomycin treatment similarly as it has been described previously [19]. Briefly, MDA-MB-436 cells were treated with 50 nM salinomycin for

72 hours when cells reached a confluency of 80%. After treatment, salinomycin was removed and replaced by fresh medium. As soon as cells recovered, they were treated again with salinomycin. After the indicated treatment cycles, the recovered salinomycin-treated cells were harvested for RNA isolation, cell lysis (protein), cytotoxicity, and migration assays.

Boyden Chamber Migration Assay

Transwells (8 μm pore size; Millipore, Darmstadt, Germany) were placed in 24-well plates containing 10% fetal calf serum in medium. Cells were suspended in 250 μl of serum-free medium, added to the top of each chamber and incubated for 18 hours. Subsequently, chambers were washed and cells were removed from the upper side of the chamber with a cotton swab. Migrated cells were fixed and stained using the cell stain solution (Chemicon International, Darmstadt, Germany). The average number of migrated cells from 15 representative fields (three replicates per condition) was counted under a phase contrast microscope. Microscopic pictures (phase contrast) show representative stained transwells.

Time-Lapse Microscopy

Time-lapse microscopy was performed using a live-cell imaging setup consisting of a microscope (Carl Zeiss MicroImaging, Jena, Germany) equipped with a Pln Apo 10×/0.45 DICII objective, a motorized scanning table, and a stage incubator at 37°C with or without CO_2. Images were captured with an AxioCamMR Rev3 camera using the Axiovision Rel 4.8 software for microscope control and data acquisition. Indicated cells were seeded in 24-well plates at a density of 50% to 70% and grown overnight. The images were captured every 15 minutes for 72 hours. Each reading was performed in triplicate. Ten random cells per well, i.e., 30 random cells per condition, were manually tracked using ImageJ [20], and the data were analyzed using the "chemotaxis and migration tool" plugin for ImageJ.

Tumor Cell Co-Culture

MCF-7 and MDA-MB-436 cells were co-cultured in Dulbecco's modified Eagle's medium/Leibovtiz's L-15 medium (1:1). For cytotoxicity assays, 5000 co-cultured cells per well were seeded in a 96-well plate and incubated overnight. Subsequently, cells were treated with 0.25 μM salinomycin, 0.25 μM doxorubicin, or the combination of 0.25 μM salinomycin and 0.25 μM doxorubicin for 72 hours. For IF, cells were seeded on coverslips at a density of 50% to 60%.

In Vitro IF

Cells were seeded on coverslips. At a confluency of 50% to 60%, cells were fixed with 4% paraformaldehyde and blocked with 10% fetal calf serum, 1% gelatin, and 0.05% Triton X-100. After permeabilizing with 0.2% Triton X-100, coverslips were incubated with primary antibodies. 4′,6-diamidino-2-phenylindole (DAPI) was used for counterstaining the nuclei, and images were captured using 63 × 1.4 oil differential interference contrast (DIC) objective of Carl Zeiss Laser Scanning Microscope LSM 510 Meta and analyzed using LSM Image Browser (Carl Zeiss). Representative images are shown.

Animal Experiments

All animal experiments were approved by the local ethical committee and performed according to the guidelines of the German law of protection of animal life.

Subcutaneous 4T1 Mouse Model

4T1 cells ($2 × 10^6$) were subcutaneously injected into the left flank of 18 female BALB/c mice (Janvier). Nine animals were treated with either mock [DMSO in phosphate-buffered saline (PBS)] or 5 mg/kg

salinomycin (2 mg/ml in DMSO stock solution was diluted in PBS) on days 3, 6, 8, 10, 13, and 15. Tumor growth was monitored for 17 days at indicated time points using a caliper. At the end of the experiment, mice were sacrificed and tumors were resected for further experiments.

Salinomycin Treatment of SpC-c-MYC Transgenic Mice

All SpC-c-MYC mice were obtained from Chitra Thakur and Ulf R. Rapp. Animals were genotyped through tail DNA at the age of 3 weeks. They have similar genetic background (>90% C57Bl/6) and were maintained heterozygous. Mice developed multifocal hyperplasias and bronchioloalveolar adenomas and carcinomas derived from alveolar type II epithelial cells within 10 to 14 months. At the average age of 7 months, mice developed early stages of tumor characterized by multifocal hyperplasias originating in the alveolar epithelium [21].

A group of 11 SpC-c-MYC mice (72 weeks old) was injected intraperitoneally every second day with 5 mg/kg salinomycin (2 mg/ml in DMSO stock solution was diluted in PBS) for 3 weeks. At the end of the experiment, mice were sacrificed and organs were collected for further analysis. Mice at the same age from the previous study by Rapp et al. [22] served as controls.

In Vivo IHC and IF

IHC (hematoxylin and eosin and marker staining) of transgenic lung tumors and subcutaneous 4T1 tumors as well as IF of 4T1 tumors were performed as described previously [22] using the primary antibodies mentioned in the Reagents section. Representative images are shown.

Statistical Analysis

All values are stated as mean ± SD unless otherwise indicated. For statistical analysis, Student's t tests were performed (*P< .5; **P< .01; ***P< .001; ****P< .0001).

Results

Sequential Salinomycin Treatment of MDA-MB-436 Breast Cancer Cells Leads to Resistance Formation and the Selection of Epithelial Cell Clones

To induce salinomycin resistance, we used the mesenchymal breast cancer cell line MDA-MB-436 and sequentially treated the cells with salinomycin. Each of the four treatment cycles was followed by a recovery phase until cells were harvested and used for further experiments. This repeated treatment of MDA-MB-436 cells with salinomycin resulted in a significantly increased resistance to salinomycin as determined by a cell viability assay (Figure 1A). Furthermore, the initially high migratory capacity of the MDA-MB-436 cells was significantly reduced in the salinomycin-resistant cells R4 (Figure 1B). Thereby, the cell morphology of salinomycin-treated cells changed from scattered spindle-shaped cells to clones growing in clusters with an epithelial-like appearance (Figure 1C). When analyzing the expression of the prominent epithelial and mesenchymal markers E-cadherin and vimentin, we observed that the mesenchymal expression pattern of these markers switched to more epithelial-like with an increase of E-cadherin and a decrease of vimentin (Figure 1, D and E). Consistent with the up-regulation of E-cadherin, the expression level of the epithelial marker miR-200c was significantly increased on salinomycin treatment (Figure 1F). In addition, we obtained a significant reduction of zeb2 mRNA, a direct target of miR-200c and an inducer of epithelial-mesenchymal transition (EMT) in mesenchymal cancer cells (Figure 1D). Thus, salinomycin treatment of the mesenchymal
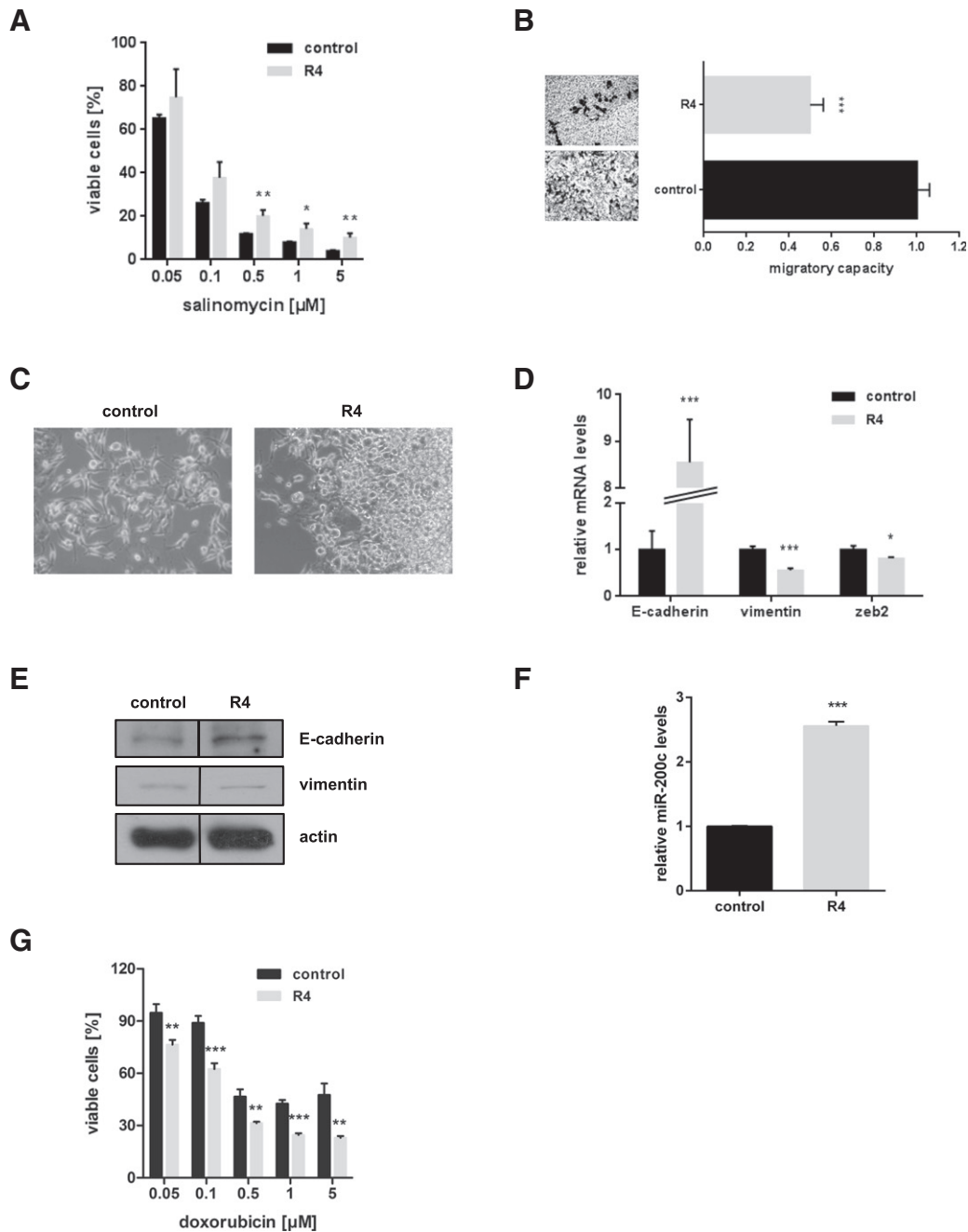
Figure 1. Sequential salinomycin treatment of MDA-MB-436 breast cancer cells leads to resistance formation and the selection of epithelial cell clones. MDA-MB-436 cells were treated in rounds with 0.05 μM salinomycin followed by a recovery phase until the next round started. Cells that had received either no (control) or four rounds of treatment (R4) were harvested for the following experiments. (A) Cytotoxicity assays of sequentially treated MDA-MB-436 cells. Salinomycin-treated (R4) as well as control cells were treated with the indicated concentrations of salinomycin. Subsequently, cell viability was assessed by the CellTiter-Glo assay. (B) Migratory capacity of control and salinomycin-treated MDA-MB-436 cells (R4). Migration was determined by the Boyden chamber assay and the migratory capacity of control cells was set to one. (C) Microscopic pictures (phase contrast) show the cell morphology of control and salinomycin-treated MDA-MB-436 cells (R4). (D) Quantitative RT-PCR analysis. Relative mRNA levels of the EMT markers E-cadherin, vimentin, and zeb2 were quantified in control and salinomycin-treated MDA-MB-436 cells (R4). (E) WB analysis. Total cell lysates of control and salinomycin-treated MDA-MB-436 cells (R4) were analyzed for the protein expression of E-cadherin and vimentin. (F) miR-200c expression of control and salinomycin-treated MDA-MB-436 cells (R4). Relative miR-200c levels were determined by quantitative RT-PCR. (G) Cytotoxicity assays of sequentially treated MDA-MB-436 cells. Salinomycin-treated (R4) as well as control cells were treated with the indicated concentrations of doxorubicin. Subsequently, cell viability was assessed by the CellTiter-Glo assay.

cancer cell line MDA-MB-436 resulted in a selection of epithelial-like cell clones as characterized by their cell morphology, epithelial and mesenchymal marker expression, and migratory capacity.

Noteworthy, these surviving epithelial-like cell clones were more resistant to salinomycin treatment and became sensitized to the classic chemotherapeutic drug doxorubicin (Figure 1*G*).

Mesenchymal-Epithelial Transition Induced by miR-200c Turns MDA-MB-436 Cells into Salinomycin-Resistant Cells

Next, we explored whether the acquisition of epithelial traits in the mesenchymal breast cancer cell line MDA-MB-436 is responsible for the increased resistance to salinomycin treatment. As miR-200c targets zeb1 and zeb2, the transcriptional repressors of E-cadherin, and thereby determines the epithelial phenotype [23–26], we used this miRNA to induce mesenchymal-epithelial transition (MET). By ectopically overexpressing miR-200c in MDA-MB-436 cells (Figure S1), we obtained a more cobblestone-shaped cell morphology (Figure 2A) and
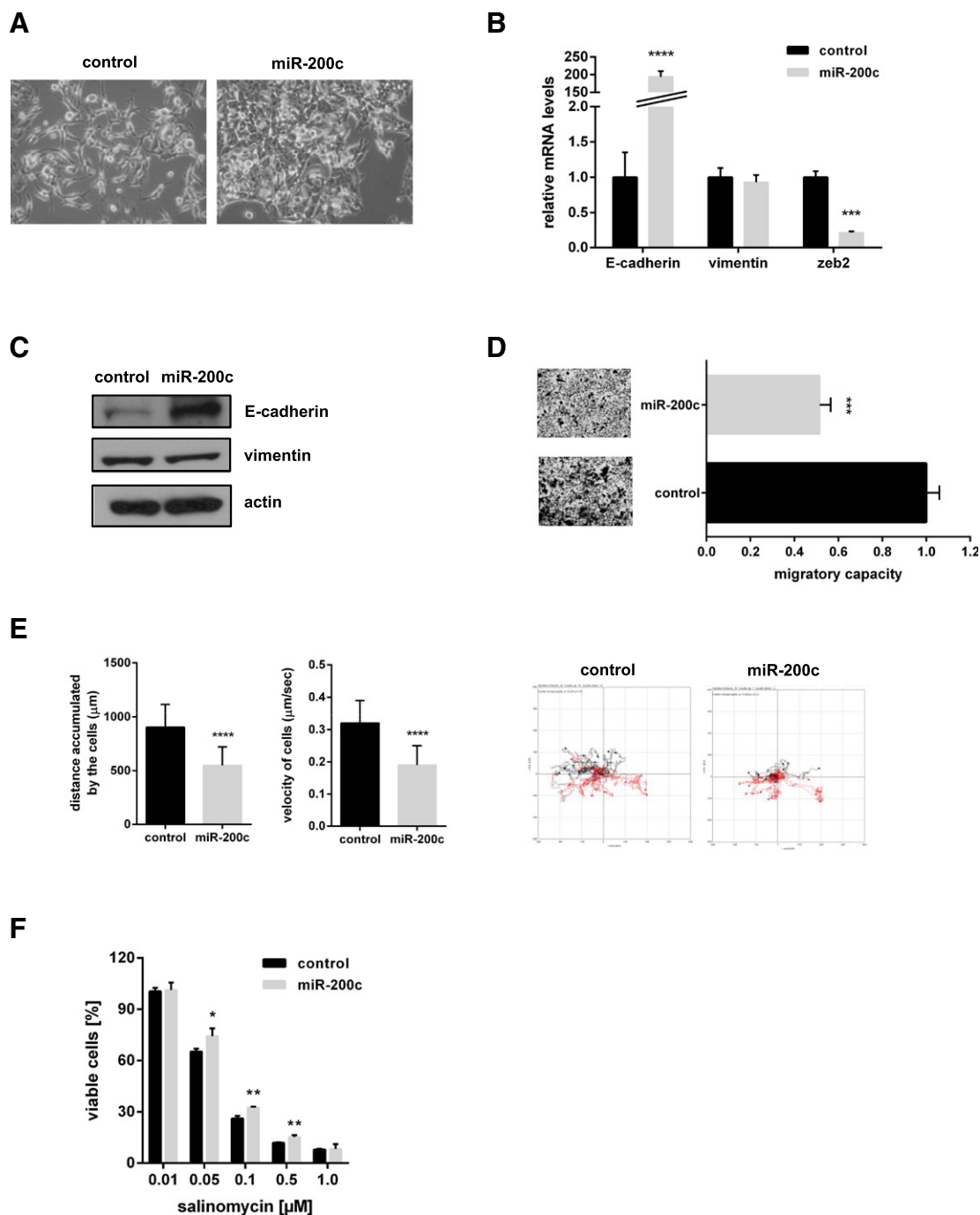

Figure 2. MET induced by miR-200c renders MDA-MB-436 cells resistant to salinomycin. (A) Cell morphology of MDA-MB-436 cells on miR-200c overexpression. Microscopic pictures (phase contrast) show the cell morphology of control and miR-200c–transfected cells. (B) Quantitative RT-PCR analysis on miR-200c overexpression in MDA-MB-436 cells. Relative mRNA levels of the EMT markers E-cadherin, vimentin, and zeb2 were quantified. (C) WB analysis on ectopic miR-200c overexpression in MDA-MB-436 cells. Total cell lysates were analyzed for the protein expression of E-cadherin and vimentin. (D) Boyden chamber migration assays of MDA-MB-436 cells overexpressing miR-200c. The number of migrated control-transfected MDA-MB-436 cells was set to a migratory capacity of one. (E) Time-lapse microscopy of MDA-MB-436 cells. Control and miR-200c–overexpressing cells were monitored using time-lapse microscopy. The accumulated distance, the velocity, and the direction of movement were analyzed. (F) Cytotoxicity assay of miR-200c–overexpressing MDA-MB-436 cells. Cells were treated with the indicated concentrations of salinomycin and cell viability was assessed using CellTiter-Glo.

an epithelial-like marker expression with increased E-cadherin and slightly reduced vimentin levels (Figure 2, B and C). In addition, mRNA expression of zeb2, the transcriptional repressor of E-cadherin and a direct target of miR-200c, was significantly reduced confirming the miR-200c–induced MET (Figure 2B). Accordingly, we obtained cells with a lower migratory capacity as determined by Boyden chamber assay (Figure 2D) and time-lapse microscopy. For the latter, we analyzed the accumulated distance, the velocity, and the direction of the movement of MDA-MB-436 cells transfected with either miR-200c or scrambled control (Figure 2E). Finally, we analyzed MDA-MB-436 cells that overexpress miR-200c in terms of their salinomycin sensitivity (Figure 2F). Of note, these cells displaying more epithelial-like properties were less susceptible to salinomycin treatment. These

findings suggest that the miR-200c–induced MET as well as a selection of epithelial-like cell clones may be an important event in the resistance formation to salinomycin treatment.

Salinomycin Is More Effective against Cancer Cells with Mesenchymal Traits

As salinomycin resistance is caused by a selection of residual epithelial-like cells or by the induction of MET by miR-200c, we investigated whether salinomycin generally affects mesenchymal cancer cells more effectively than epithelial cancer cells. Therefore, we characterized several breast and lung cancer cell lines in terms of their epithelial or mesenchymal phenotypes, i.e., their cell morphology, epithelial and mesenchymal marker expression, and migratory capacity.
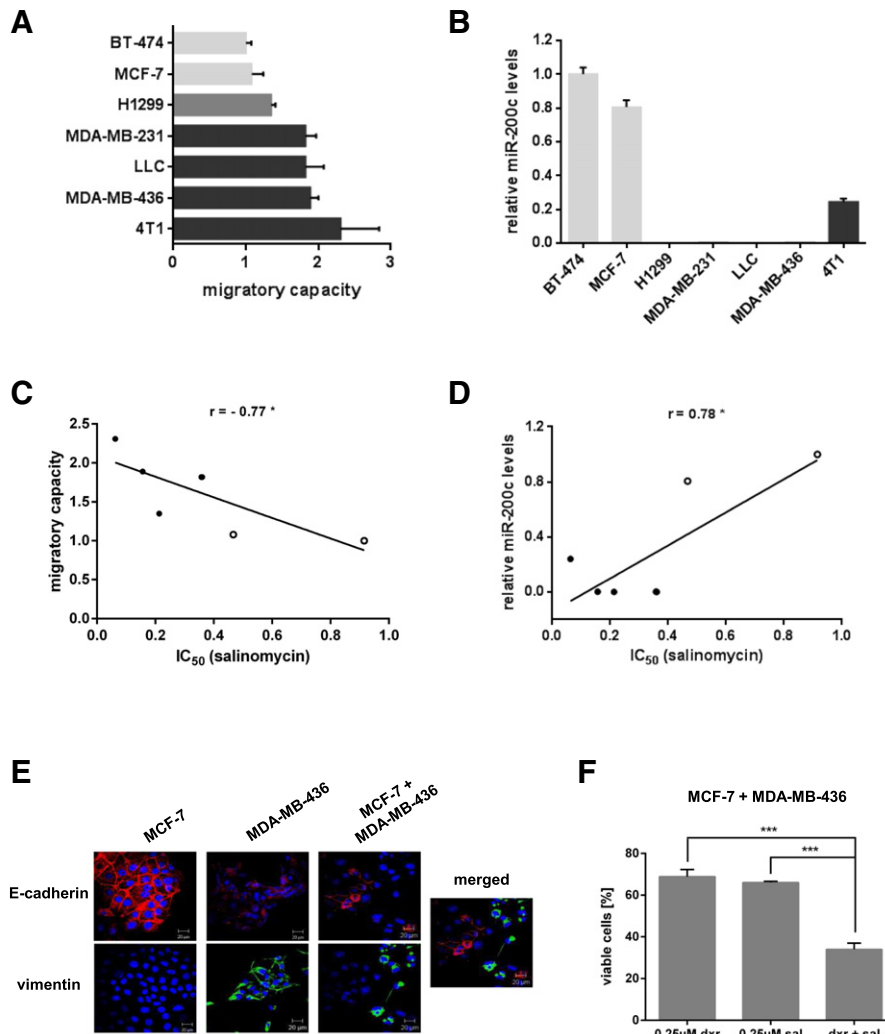
Figure 3. Salinomycin is more effective against cancer cells with mesenchymal traits. (A) Boyden chamber migration assays of different breast and lung cancer cell lines. The number of migrated BT-474 cells was set to a migratory capacity of one, and the remaining cell lines were normalized as fold of the migratory capacity of BT-474 cells. (B) miR-200c expression in the different cancer cell lines. Relative miR-200c levels were determined by quantitative RT-PCR. (C) Correlation between migratory capacity and susceptibility to salinomycin. IC_{50} values for salinomycin were determined in the panel of breast cancer cells by the CellTiter-Glo assay and correlated with the migratory capacity of the respective cell lines (Pearson $r = -0.77$). Open circles represent the epithelial cell lines BT-474 and MCF-7. (D) Correlation between relative miR-200c expression and susceptibility to salinomycin. A Pearson correlation was carried out to compare the sensitivity to salinomycin with the relative miR-200c expression of the respective cell lines (Pearson $r = 0.78$). Open circles represent the epithelial cell lines BT-474 and MCF-7. (E) Microscopy of single and co-cultured MCF-7 and/or MDA-MB-436 cells. IF pictures for E-cadherin (red) and vimentin (green) were taken either from MCF-7, MDA-MB-436, or MCF-7 + MDA-MB-436. Nuclei were stained with DAPI (blue). (F) Treatment of co-cultured MCF-7 and MDA-MB-436 cells. Co-cultured cells were treated with the indicated concentrations of salinomycin (sal) and/or doxorubicin (dox).

Table 1. Migratory Capacity, Relative miR-200c Expression, and Salinomycin Susceptibility in the Different Cancer Cell Lines

	4T1	MDA-MB-436	LLC	MDA-MB-231	H1299	MCF-7	BT-474
Migratory capacity	2.31	1.89		1.82	1.82	1.35	1.08	1.00
Relative miR-200c expression	0.241	0.002	0.000	0.002	0.000	0.807	1.000
IC_{50} (salinomycin) [μM]	0.06	0.16	0.36	0.36	0.21	0.47	0.92

The migratory capacity was determined by Boyden chamber assays, the relative miR-200c levels were determined by quantitative RT-PCR, and the IC_{50} values for salinomycin were assessed by the CellTiter-Glo assay using several concentrations of salinomycin.

The migratory potential of a panel of breast (BT-474, MCF-7, MDA-MB-231, MDA-MB-436, and 4T1) and lung (H1299 and LLC) cancer cell lines was determined by Boyden chamber assays (Figure 3A).

Accordingly, cell lines with an increased migratory capacity displayed a high vimentin and, in most cases, a low E-cadherin expression on both the protein and mRNA levels (Figure S2). This was in line with their mesenchymal spindle-shaped cell morphology (Figure S2). 4T1 cells, however, displayed high vimentin and significant E-cadherin levels representing a heterogeneous cell population consisting of mesenchymal and epithelial cells as determined by IF staining (Figure S3), i.e., cells that highly express vimentin have rather low levels of E-cadherin and *vice versa*. Finally, the expression of miR-200c as a key regulator of EMT was investigated in the panel of cancer cell lines. In accordance with the expression of the other markers, miR-200c levels were high in epithelial, low in mesenchymal, and medium in 4T1 cells (Figure 3B).

To examine the differential sensitivity of these epithelial and mesenchymal cancer cell lines to salinomycin, the IC_{50} value for each cell line was determined and correlated with the respective migratory
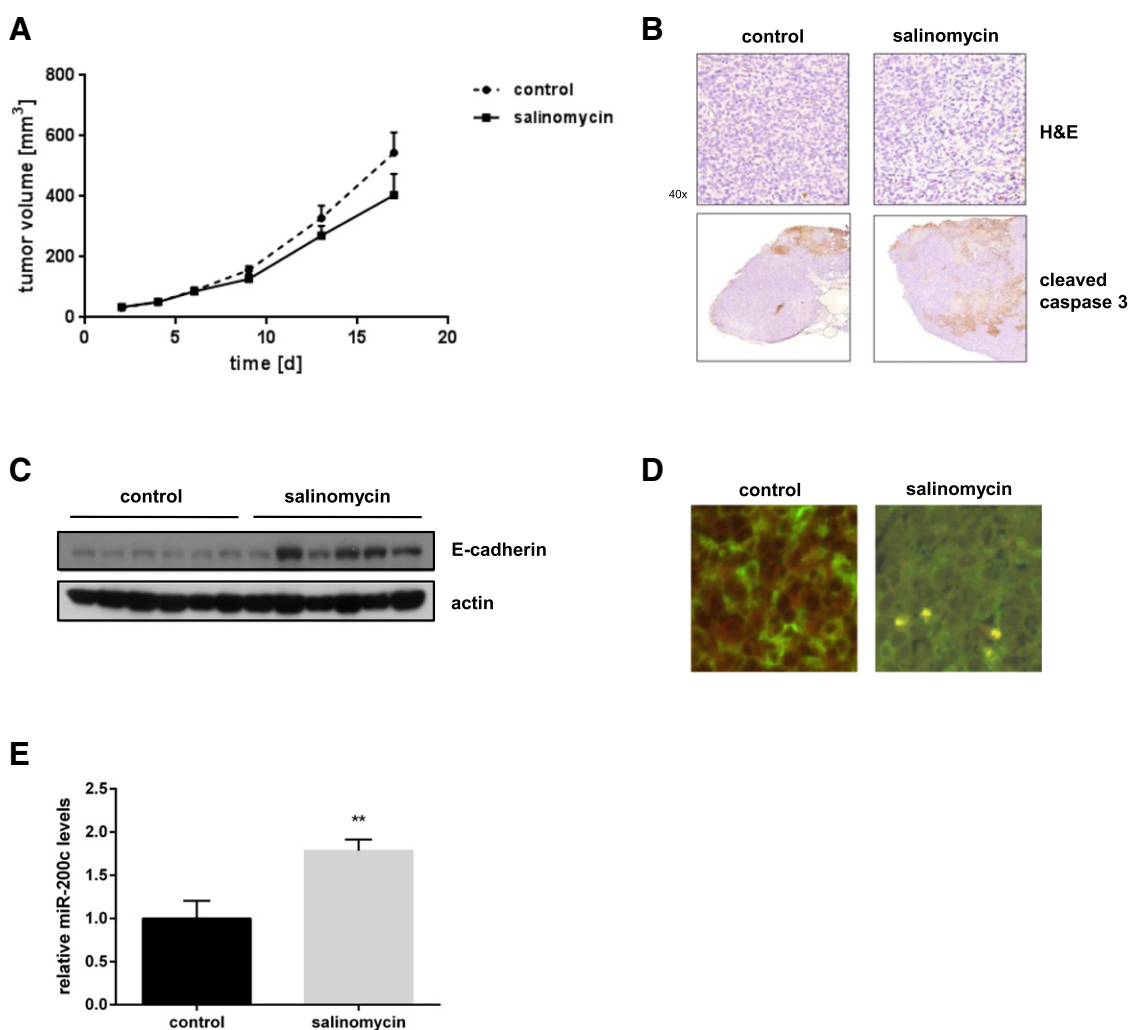
Figure 4. Salinomycin treatment selects tumor cells with increased epithelial marker expression in a syngeneic mouse tumor model. (A) Tumor growth of subcutaneous 4T1 tumors. 4T1 cells (2×10^6) were subcutaneously injected into the right flank of nine female BALB/c mice per group. Animals were treated with either mock (control) or 5 mg/kg salinomycin on days 3, 6, 8, 10, 13, and 15. Tumor growth was monitored for 17 days at the indicated time points using a caliper and depicted as tumor volume (mm^3). (B) IHC of subcutaneous 4T1 tumors. On day 17, mice were sacrificed and tumors were resected. Sections of paraffin-embedded control and salinomycin-treated tumors were used for IHC and stained for hematoxylin and eosin and cleaved caspase 3. (C) WB analysis of 4T1 tumors. Lysates from representative control and salinomycin-treated tumors were analyzed for the E-cadherin protein expression. (D) IF of 4T1 tumors. Respective tumor sections were stained for E-cadherin (green) and vimentin (red). (E) miR-200c expression in 4T1 tumors. Relative miR-200c levels of salinomycin- and mock-treated (control) 4T1 tumors were determined by quantitative RT-PCR. (mean ± SEM).

capacity or miR-200c expression as makers for EMT. Thereby, mesenchymal cell lines with a high migratory potential were rather sensitive to salinomycin, whereas epithelial cell lines with a low migratory capacity were more resistant to salinomycin (Pearson $r= -0.77$; Figure 3C). Accordingly, miR-200c expression directly correlated with salinomycin resistance (Pearson $r= 0.78$; Figure 3D). A numerical table of the different salinomycin IC_{50} values, migratory capacities, and relative miR-200c expression levels is provided in Table 1. These results emphasize the higher efficacy of salinomycin against mesenchymal cancer cells. Taking these findings and the increased doxorubicin sensitivity after salinomycin treatment (Figure 1G) into account, we hypothesized that combined treatment of salinomycin and doxorubicin will have additive effects on heterogeneous tumor cell populations. We therefore co-cultured the epithelial, non-migratory breast cancer cell line MCF-7 and the mesenchymal, highly migratory breast cancer cell line MDA-MB-436. The obtained cell mix roughly reflects the cellular heterogeneity in tumors, comprising epithelial and mesenchymal cells as shown by IF staining of E-cadherin and vimentin (Figure 3E). Single treatment as well as combinatorial treatment with doxorubicin and salinomycin revealed a beneficial effect of the combination confirming the selective efficacy of the respective drug on the different cell types (Figure 3F).

Salinomycin Treatment Selects Tumor Cells with Increased Epithelial Marker Expression in a Syngeneic Mouse Tumor Model

Salinomycin was demonstrated to be effective in different xenograft mouse tumor models [8,12,14]. Here, we evaluated the potential of salinomycin to target mesenchymal cancer cells and thus to induce a more epithelial-like phenotype *in vivo*. Therefore, we used the murine breast cancer cell line 4T1, which *per se* comprises a heterogeneous cell population exhibiting both an epithelial (E-cadherin) and a mesenchymal (vimentin) marker expression (Figure S3). 4T1 cells were subcutaneously injected into BALB/c mice and treated with either salinomycin or mock (control) every second or third day. A slight effect of salinomycin treatment on tumor growth was observed (Figure 4A), which can be explained by an increased apoptosis as determined by IHC of cleaved caspase 3 (Figure 4B). Of note, consistent with the *in vitro* results of

salinomycin-treated MDA-MB-436 cells, salinomycin-treated tumors displayed elevated E-cadherin protein levels as determined by WB analysis (Figure 4C). IF staining of untreated 4T1 tumor sections revealed a heterogeneous cell population consisting of either E-cadherin–positive or vimentin-positive cells. The latter disappeared after salinomycin treatment resulting in an epithelial-like tumor with considerable E-cadherin expression (Figure 4D), emphasizing the selective killing of mesenchymal-like cancer cells. Moreover, miR-200c expression was significantly increased on salinomycin treatment (Figure 4E). On the basis of these observations, we raised the question of whether an up-regulation of miR-200c was able to inhibit the migration of 4T1 cells as these cells already display a medium expression of miR-200c. Therefore, we investigated the migratory capacity of 4T1 cells on miR-200c overexpression. Boyden chamber assay and time-lapse microscopy (Figure S4) demonstrated that overexpression of miR-200c significantly reduced the migratory capacity as well as the accumulated distance, the velocity, and the movement of the miR-200c medium-expressing 4T1 cells, suggesting an additional beneficial effect of salinomycin treatment.

Residual Tumor Cells of an SpC-c-MYC Transgenic Mouse Tumor Model Display Enhanced Epithelial Marker Expression

To investigate the selectivity of salinomycin treatment on mesenchymal tumor cells in a model based on spontaneous carcinogenesis, we used the c-MYC–driven transgenic mouse model of non–small cell lung cancer, which has been previously described by Rapp et al. [22]. The animals received nine treatments with salinomycin every second day. IHC of salinomycin-treated and control SpC-c-MYC mice displayed an epithelial-like expression pattern with increased E-cadherin levels on salinomycin treatment (Figure 5A). Vimentin expression was low and could not be significantly downregulated (Figure 5B). Consistent with the syngeneic mouse model, salinomycin-treated lung tumors showed increased PARP cleavage, indicating augmented apoptosis on treatment (Figure 5C). Hence, salinomycin treatment of subcutaneous 4T1 tumors as well as of transgenic SpC-c-MYC lung tumors led to a selection of epithelial-like tumor cells, underpinning this resistance mechanism after long-term application of salinomycin.
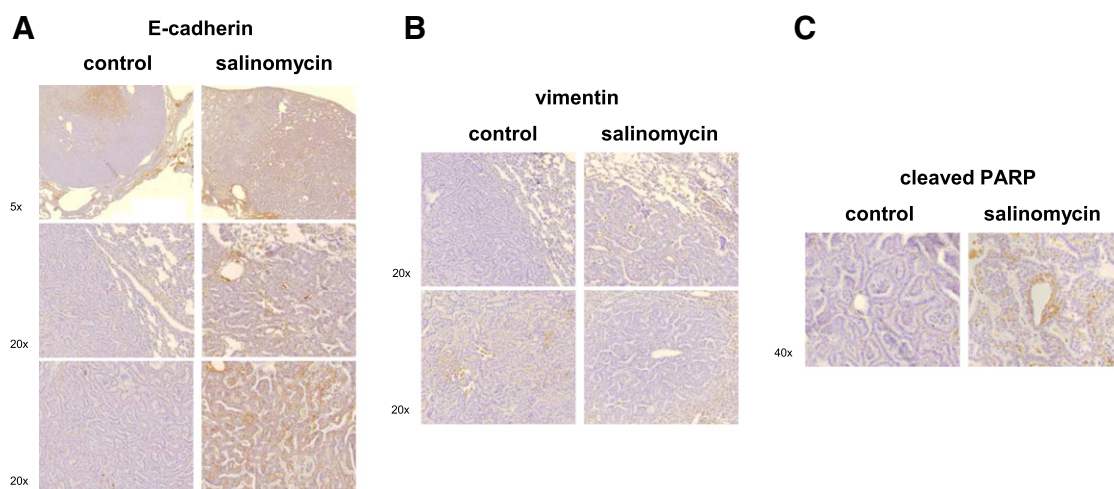
Figure 5. Residual tumor cells of an SpC-c-MYC transgenic mouse tumor model display enhanced epithelial marker expression. IHC of lung tumors obtained from tumor-bearing transgenic mice. SpC-c-MYC mice at the age of 72 weeks received 12 treatments with 5 mg/kg salinomycin every second day. Untreated tumor-bearing SpC-c-MYC mice at nearly the same age were used as a control group. Paraffin-embedded sections of tumor-bearing lungs were stained for either (A) E-cadherin, (B) vimentin, or (C) cleaved Poly(ADP-ribose)-Polymerase (PARP).

Discussion

It has been suggested that intratumoral heterogeneity derived from genetic and non-genetic alterations can remarkably influence clinically important events, such as metastasis formation and therapy resistance [27,28]. This implicates that a tumor comprises different cellular phenotypes, among them migratory, mesenchymal, more chemoresistant cells, as well as non-migratory, epithelial, commonly chemosensitive cells. Developing novel therapeutic strategies for targeting all the different cell populations within a tumor is crucial for a successful cancer therapy. Hence, the discovery of the CSC-specific drug salinomycin raised hope for improved treatment options for patients with cancer by targeting a chemoresistant subpopulation of tumor cells.

While the occurrence of resistance to classic chemotherapy and targeted cancer therapies is well described, very little is known about the resistance formation to salinomycin. Thus, the characterization of the resistance mechanisms of salinomycin is of particular interest. The up-regulation of growth factor receptors or prominent cellular survival pathways is thought to contribute to an enhanced cell survival as an immediate effect on salinomycin treatment. For instance, the activation of Akt has been reported as an immediate response to salinomycin treatment leading to a reduction of salinomycin-induced apoptosis [29]. However, in contrast to such immediate resistance responses, we report here an acquired resistance of cancer cells on long-term salinomycin treatment. We demonstrated that sequential salinomycin treatment resulted in a selection of epithelial-like cell clones with increased E-cadherin expression, elevated miR-200c levels, and decreased cell motility. Most notably, this phenotypic switch was accompanied by an increased resistance to salinomycin treatment. We furthermore showed that cancer cells in an epithelial state, i.e., cells with a high epithelial marker expression such as miR-200c and a low migratory capability, generally display an enhanced resistance to salinomycin as compared to mesenchymal cancer cells. Accordingly, it has been reported that mesenchymal cancer cells are dedifferentiated and therefore exhibit properties of CSC [30], which are known to be susceptible to salinomycin treatment. Noteworthy, we showed that long-term salinomycin treatment resulted in the acquisition of epithelial traits in the syngeneic 4T1 mouse tumor model and in the SpC-c-MYC transgenic mouse model for non–small cell lung cancer, indicating the occurrence of salinomycin resistance also *in vivo*.

We support the hypothesis that genetic instability and clonal selection [31] play an essential role in long-term resistance formation in general. In accordance with this model, long-term salinomycin treatment determines surviving clones, which exhibit epithelial properties and are less sensitive to the respective treatment. The selection of epithelial E-cadherin–positive cells in heterogeneous 4T1 tumors on salinomycin treatment gives further evidence for clonal evolution as a resistance mechanism. As suggested by recent publications [32–34], epithelial cells may have a higher capability than mesenchymal cells to initiate autophagy and thereby to circumvent salinomycin-induced cytotoxicity, hence explaining the differential salinomycin susceptibility of these two cell types.

EMT is well known to play a crucial role in tumor progression and therapy resistance [35]. In particular, the resistance to classic chemotherapy as well as to targeted therapies, such as gefitinib or erlotinib, has been ascribed to an induction of EMT in several cancer types [19,36–38]. Here, we describe the opposite phenomenon of an increase of epithelial traits on salinomycin treatment. Therefore, this long-term resistance formation to salinomycin treatment does not necessarily have to be a disadvantage for cancer therapy. Especially, the up-regulation of miR-200c represents a favorable effect of salinomycin

treatment as miR-200c hampers migration and metastasis by preventing EMT [23–26,39–41] and modulating migration-relevant target genes [42,43]. Accordingly, recent studies demonstrated that salinomycin hampered metastasis formation of lung and breast cancer cells in mice without significant effects on the primary tumor growth [44,45]. Moreover, it has been shown that an increased expression of miR-200c improves the susceptibility to classic chemotherapeutics [19,36,46–51] indicating that acquiring resistance to salinomycin may be beneficial for the treatment with conventional chemotherapy.

Hence, salinomycin may antagonize tumor progression by reverting chemotherapy-induced EMT, which is known to be strongly associated with metastasis formation and therapy resistance. Salinomycin treatment thereby leads to less aggressive cancer cells and tumors in terms of lower migratory capacity, less metastasis, and higher susceptibility to classic chemotherapy. Salinomycin resistance could therefore become exploited for conventional cancer therapy in combination with classic chemotherapy, eventually rendering cancer better controllable.

Acknowledgments

Appendix A. Supplementary data

Supplementary data to this article can be found online at http://dx.doi.org/10.1016/j.tranon.2014.09.002.

References

[1] Coley HM (2008). Mechanisms and strategies to overcome chemotherapy resistance in metastatic breast cancer. *Cancer Treat Rev* **34**, 378–390.

[2] Gonzalez-Angulo AM, Morales-Vasquez F, and Hortobagyi GN (2007). Overview of resistance to systemic therapy in patients with breast cancer. *Adv Exp Med Biol* **608**, 1–22.

[3] O'Driscoll L and Clynes M (2006). Biomarkers and multiple drug resistance in breast cancer. *Curr Cancer Drug Targets* **6**, 365–384.

[4] Raguz S and Yagüe E (2008). Resistance to chemotherapy: new treatments and novel insights into an old problem. *Br J Cancer* **99**, 387–391.

[5] De Sousa EMF, Vermeulen L, Fessler E, and Medema JP (2013). Cancer heterogeneity—a multifaceted view. *EMBO Rep* **14**, 686–695.

[6] Marjanovic ND, Weinberg RA, and Chaffer CL (2013). Cell plasticity and heterogeneity in cancer. *Clin Chem* **59**, 168–179.

[7] Zhang XC, Xu C, Mitchell RM, Zhang B, Zhao D, Li Y, Huang X, Fan W, Wang H, and Lerma LA, et al (2013). Tumor evolution and intratumor heterogeneity of an oropharyngeal squamous cell carcinoma revealed by whole-genome sequencing. *Neoplasia* **15**, 1371–1378.

[8] Gupta PB, Onder TT, Jiang G, Tao K, Kuperwasser C, Weinberg RA, and Lander ES (2009). Identification of selective inhibitors of cancer stem cells by high-throughput screening. *Cell* **138**, 645–659.

[9] Naujokat C and Steinhart R (2012). Salinomycin as a drug for targeting human cancer stem cells. *J Biomed Biotechnol* **2012**, 950658.

[10] Ketola K, Hilvo M, Hyötyläinen T, Vuoristo A, Ruskeepää AL, Orešič M, Kallioniemi O, and Iljin K (2012). Salinomycin inhibits prostate cancer growth and migration via induction of oxidative stress. *Br J Cancer* **106**, 99–106.

[11] Koo KH, Kim H, Bae YK, Kim K, Park BK, Lee CH, and Kim YN (2013). Salinomycin induces cell death via inactivation of Stat3 and downregulation of Skp2. *Cell Death Dis* **4**, e693.

[12] Wang F, He L, Dai WQ, Xu YP, Wu D, Lin CL, Wu SM, Cheng P, Zhang Y, and Shen M, et al (2012). Salinomycin inhibits proliferation and induces apoptosis of human hepatocellular carcinoma cells in vitro and in vivo. *PLoS One* **7**, e50638.

[13] Zhou J, Li P, Xue X, He S, Kuang Y, Zhao H, Chen S, Zhi Q, and Guo X (2013). Salinomycin induces apoptosis in cisplatin-resistant colorectal cancer cells by accumulation of reactive oxygen species. *Toxicol Lett* **222**, 139–145.

[14] Zhang B, Wang X, Cai F, Chen W, Loesch U, and Zhong XY (2013). Antitumor properties of salinomycin on cisplatin-resistant human ovarian cancer cells in vitro and in vivo: involvement of p38 MAPK activation. *Oncol Rep* **29**, 1371–1378.

[15] Parajuli B, Shin SJ, Kwon SH, Cha SD, Chung R, Park WJ, Lee HG, and Cho CH (2013). Salinomycin induces apoptosis via death receptor-5 up-regulation in cisplatin-resistant ovarian cancer cells. *Anticancer Res* **33**, 1457–1462.

[16] Fuchs D, Daniel V, Sadeghi M, Opelz G, and Naujokat C (2010). Salinomycin overcomes ABC transporter-mediated multidrug and apoptosis resistance in human leukemia stem cell-like KG-1a cells. *Biochem Biophys Res Commun* **394**, 1098–1104.

[17] Kim JH, Yoo HI, Kang HS, Ro J, and Yoon S (2012). Salinomycin sensitizes antimitotic drugs-treated cancer cells by increasing apoptosis via the prevention of G2 arrest. *Biochem Biophys Res Commun* **418**, 98–103.

[18] Kim JH, Chae M, Kim WK, Kim YJ, Kang HS, Kim HS, and Yoon S (2011). Salinomycin sensitizes cancer cells to the effects of doxorubicin and etoposide treatment by increasing DNA damage and reducing p21 protein. *Br J Pharmacol* **162**, 773–784.

[19] Kopp F, Oak PS, Wagner E, and Roidl A (2012). miR-200c sensitizes breast cancer cells to doxorubicin treatment by decreasing TrkB and Bmi1 expression. *PLoS One* **7**, e50469.

[20] Rasband WS (1997–2008). ImageJ, U.S. National Institutes of Health, Bethesda, Maryland, USA. Editor (ed)^(eds): City.

[21] Ehrhardt A, Bartels T, Klocke R, Paul D, and Halter R (2003). Increased susceptibility to the tobacco carcinogen 4-(methylnitrosamino)-1-(3-pyridyl)-1-butanone in transgenic mice overexpressing c-myc and epidermal growth factor in alveolar type II cells. *J Cancer Res Clin Oncol* **129**, 71–75.

[22] Rapp UR, Korn C, Ceteci F, Karreman C, Luetkenhaus K, Serafin V, Zanucco E, Castro I, and Potapenko T (2009). MYC is a metastasis gene for non-small-cell lung cancer. *PLoS One* **4**, e6029.

[23] Burk U, Schubert J, Wellner U, Schmalhofer O, Vincan E, Spaderna S, and Brabletz T (2008). A reciprocal repression between ZEB1 and members of the miR-200 family promotes EMT and invasion in cancer cells. *EMBO Rep* **9**, 582–589.

[24] Gregory PA, Bert AG, Paterson EL, Barry SC, Tsykin A, Farshid G, Vadas MA, Khew-Goodall Y, and Goodall GJ (2008). The miR-200 family and miR-205 regulate epithelial to mesenchymal transition by targeting ZEB1 and SIP1. *Nat Cell Biol* **10**, 593–601.

[25] Korpal M, Lee ES, Hu G, and Kang Y (2008). The miR-200 family inhibits epithelial-mesenchymal transition and cancer cell migration by direct targeting of E-cadherin transcriptional repressors ZEB1 and ZEB2. *J Biol Chem* **283**, 14910–14914.

[26] Park SM, Gaur AB, Lengyel E, and Peter ME (2008). The miR-200 family determines the epithelial phenotype of cancer cells by targeting the E-cadherin repressors ZEB1 and ZEB2. *Genes Dev* **22**, 894–907.

[27] Marusyk A, Almendro V, and Polyak K (2012). Intra-tumour heterogeneity: a looking glass for cancer? *Nat Rev Cancer* **12**, 323–334.

[28] Rehemtulla A (2013). Cancer subclonal genetic architecture as a key to personalized medicine. *Neoplasia* **15**, 1410–1420.

[29] Kim JH, Choi AR, Kim YK, Kim HS, and Yoon S (2013). Low amount of salinomycin greatly increases Akt activation, but reduces activated p70S6K levels. *Int J Mol Sci* **14**, 17304–17318.

[30] Mani SA, Guo W, Liao MJ, Eaton EN, Ayyanan A, Zhou AY, Brooks M, Reinhard F, Zhang CC, and Shipitsin M, et al (2008). The epithelial-mesenchymal transition generates cells with properties of stem cells. *Cell* **133**, 704–715.

[31] Cahill DP, Kinzler KW, Vogelstein B, and Lengauer C (1999). Genetic instability and darwinian selection in tumours. *Trends Cell Biol* **9**, M57–M60.

[32] Li T, Su L, Zhong N, Hao X, Zhong D, Singhal S, and Liu X (2013). Salinomycin induces cell death with autophagy through activation of endoplasmic reticulum stress in human cancer cells. *Autophagy*, 9.

[33] Jangamreddy JR, Ghavami S, Grabarek J, Kratz G, Wiechec E, Fredriksson BA, Rao RK, Cieslar-Pobuda A, Panigrahi S, and Los MJ (2013). Salinomycin induces activation of autophagy, mitophagy and affects mitochondrial polarity: differences between primary and cancer cells. *Biochim Biophys Acta* **1833**, 2057–2069.

[34] Verdoodt B, Vogt M, Schmitz I, Liffers ST, Tannapfel A, and Mirmohammadsadegh A (2012). Salinomycin induces autophagy in colon and breast cancer cells with concomitant generation of reactive oxygen species. *PLoS One* **7**, e44132.

[35] Polyak K and Weinberg RA (2009). Transitions between epithelial and mesenchymal states: acquisition of malignant and stem cell traits. *Nat Rev Cancer* **9**, 265–273.

[36] Bryant JL, Britson J, Balko JM, Willian M, Timmons R, Frolov A, and Black EP (2012). A microRNA gene expression signature predicts response to erlotinib in epithelial cancer cell lines and targets EMT. *Br J Cancer* **106**, 148–156.

[37] Maseki S, Ijichi K, Tanaka H, Fujii M, Hasegawa Y, Ogawa T, Murakami S, Kondo E, and Nakanishi H (2012). Acquisition of EMT phenotype in the gefitinib-resistant cells of a head and neck squamous cell carcinoma cell line through Akt/GSK-3β/snail signalling pathway. *Br J Cancer* **106**, 1196–1204.

[38] Zhang W, Feng M, Zheng G, Chen Y, Wang X, Pen B, Yin J, Yu Y, and He Z (2012). Chemoresistance to 5-fluorouracil induces epithelial-mesenchymal transition via up-regulation of Snail in MCF7 human breast cancer cells. *Biochem Biophys Res Commun* **417**, 679–685.

[39] Paterson EL, Kazenwadel J, Bert AG, Khew-Goodall Y, Ruszkiewicz A, and Goodall GJ (2013). Down-regulation of the miRNA-200 family at the invasive front of colorectal cancers with degraded basement membrane indicates EMT is involved in cancer progression. *Neoplasia* **15**, 180–191.

[40] Gibbons DL, Lin W, Creighton CJ, Rizvi ZH, Gregory PA, Goodall GJ, Thilaganathan N, Du L, Zhang Y, and Pertsemlidis A, et al (2009). Contextual extracellular cues promote tumor cell EMT and metastasis by regulating miR-200 family expression. *Genes Dev* **23**, 2140–2151.

[41] Olson P, Lu J, Zhang H, Shai A, Chun MG, Wang Y, Libutti SK, Nakakura EK, Golub TR, and Hanahan D (2009). MicroRNA dynamics in the stages of tumorigenesis correlate with hallmark capabilities of cancer. *Genes Dev* **23**, 2152–2165.

[42] Howe EN, Cochrane DR, and Richer JK (2011). Targets of miR-200c mediate suppression of cell motility and anoikis resistance. *Breast Cancer Res* **13**, R45.

[43] Jurmeister S, Baumann M, Balwierz A, Keklikoglou I, Ward A, Uhlmann S, Zhang JD, Wiemann S, and Sahin Ö (2012). MicroRNA-200c represses migration and invasion of breast cancer cells by targeting actin-regulatory proteins FHOD1 and PPM1F. *Mol Cell Biol* **32**, 633–651.

[44] Kopp F, Hermawan A, Oak PS, Herrmann A, Wagner E, and Roidl A (2014). Salinomycin treatment reduces metastatic tumor burden by hampering cancer cell migration. *Mol Cancer* **13**, 16.

[45] Larzabal L, El-Nikhely N, Redrado M, Seeger W, Savai R, and Calvo A (2013). Differential effects of drugs targeting cancer stem cell (CSC) and non-CSC populations on lung primary tumors and metastasis. *PLoS One* **8**, e79798.

[46] Cochrane DR, Howe EN, Spoelstra NS, and Richer JK (2010). Loss of miR-200c: a marker of aggressiveness and chemoresistance in female reproductive cancers. *J Oncol* **2010**, 821717.

[47] Cochrane DR, Spoelstra NS, Howe EN, Nordeen SK, and Richer JK (2009). MicroRNA-200c mitigates invasiveness and restores sensitivity to microtubule-targeting chemotherapeutic agents. *Mol Cancer Ther* **8**, 1055–1066.

[48] Liu S, Tetzlaff MT, Cui R, and Xu X (2012). miR-200c inhibits melanoma progression and drug resistance through down-regulation of BMI-1. *Am J Pathol* **181**, 1823–1835.

[49] Pogribny IP, Filkowski JN, Tryndyak VP, Golubov A, Shpyleva SI, and Kovalchuk O (2010). Alterations of microRNAs and their targets are associated with acquired resistance of MCF-7 breast cancer cells to cisplatin. *Int J Cancer* **127**, 1785–1794.

[50] Tryndyak VP, Beland FA, and Pogribny IP (2010). E-cadherin transcriptional down-regulation by epigenetic and microRNA-200 family alterations is related to mesenchymal and drug-resistant phenotypes in human breast cancer cells. *Int J Cancer* **126**, 2575–2583.

[51] Kopp F, Wagner E, and Roidl A (2014). The proto-oncogene KRAS is targeted by miR-200c. *Oncotarget* **5**, 185–195.